

# Noise Suppression and Performance Enhancement Field-Oriented-Controlled Induction Machine Drive System with Model-Predictive-Controllers

Vivek Pahwa

Department of Electrical and Electronics Engineering, University Institute of Engineering and Technology, Panjab University, Chandigarh, India.

## ABSTRACT

This study presents an innovative solution to alleviate the detrimental effects of noise in the speed sensor of a field-oriented-controlled induction motor drive system. The proposed methodology employs two model predictive controllers; one is utilized for a reference-torque generator, while the other is implemented for the reference-flux. The former controller guarantees the stability of the system, whereas the latter suppresses the noise of the drive system. This investigation illustrates the efficacy and superiority of these model predictive controllers by contrasting their performance with that of conventional proportional-integral controllers.

**Keywords:** Induction Machine, Model Predictive Controller (MPC), Proportional Integral (PI) Controller, Noise, Field Oriented Control

*SAMRIDDHI : A Journal of Physical Sciences, Engineering and Technology* (2023); DOI: 10.18090/samriddhi.v15i01.34

## INTRODUCTION

Sophisticated speed regulation of induction motors holds paramount significance in industrial applications. This can be achieved through flux decoupling, which facilitates the independent management of the motor's flux and torque components. Such a capability enables precise motor control, enhances dynamic responsiveness, and augments efficiency across a diverse array of applications. Field-Oriented-Control (FOC) and Direct-Torque-Control (DTC) are the two predominant methodologies utilized for the decoupling of flux and torque in induction motors. FOC is regarded as more straightforward to implement in comparison to the intricate DTC, thus rendering it the preferred choice of the two [1-2].

Field-Oriented-Control can be realized through stator flux-oriented control, rotor flux-oriented control, or air gap flux-oriented control. The stator flux-oriented control emphasizes the regulation of the stator flux component, whereas rotor flux-oriented control is concerned with the management of the rotor flux component. Air gap flux-oriented control, on the other hand, is predicated on the modulation of the air gap flux within the induction motor. Among these methodologies, Rotor Flux Oriented Control is favored due to its inherent capability to provide a natural decoupling effect [3].

FOC employs reference-frame theory to transmute the variables and equations from the stationary abc reference frame to the rotating abc reference frame, subsequently transitioning to the rotating d-q reference frame. The d-q reference frame rotates in synchrony with the rotor flux of

**Corresponding Author:** Vivek Pahwa, Department of Electrical and Electronics Engineering, University Institute of Engineering and Technology, Panjab University, Chandigarh, India., e-mail: v1974pahwa@gmail.com

**How to cite this article:** Pahwa, V. (2023). Noise Suppression and Performance Enhancement Field-Oriented-Controlled Induction Machine Drive System with Model-Predictive-Controllers. *SAMRIDDHI : A Journal of Physical Sciences, Engineering and Technology*, 15(1), 192-199.

**Source of support:** Nil

**Conflict of interest:** None

the machine, rendering it instrumental for the analysis and management of the machine's dynamics [4-7].

Speed sensors are employed to provide precise feedback for Field-Oriented Control (FOC) in induction motors. The various types of sensors utilized include Hall Effect Sensors [8], Optical Encoders [9], and DC Tachometers [10]. These speed sensors furnish critical information regarding the rotational velocity of the motor shaft, thereby facilitating meticulous regulation of the motor's speed and positioning. However, intrinsic and undesirable factors such as aging and vibrations detrimentally impact the feedback signals derived from these sensors for speed and position measurement. They introduce noise and disturbances that compromise the quality and reliability of the feedback signal, ultimately leading to a deterioration of the system's output [11]. This noise engenders motor performance that is far from optimal.

Owing to their inherent simplicity, transfer function-based control strategies such as Proportional Integral (PI) control [12], Advanced PI control [13], and Sliding Mode Control [14] are employed in Field Oriented Control (FOC) for induction motor drives. However, these methodologies exhibit limitations in effectively managing noise and disturbances within the system. While the integration of an external Kalman filter with these controllers is a conceivable approach, it does not represent the most optimal solution, as it introduces additional complexity, rendering the system cumbersome. This integration incurs a computational burden and may necessitate further tuning and implementation efforts.

In contrast to the aforementioned controllers, another controller that has gained prominence in recent years is the Model Predictive Controller (MPC). It adeptly mitigates system noise through its integrated Kalman filtering mechanism [15]. Furthermore, it employs sophisticated optimization techniques [16] to ascertain the optimal control actions that minimize a specified cost function while adhering to system constraints. The optimization paradigm of MPC facilitates dynamic and real-time decision-making, empowering the controller to adapt to evolving conditions and achieve enhanced performance [17].

Therefore, in this study, two Model Predictive Controllers (MPCs) have been employed in distinct control loops of the three-phase field-oriented controlled Induction Machine drive system. One MPC functions within the control loop that generates the reference flux, while the other operates in the loop responsible for generating the reference torque. The MPC in the reference flux loop enhances overall performance. Conversely, the MPC in the reference torque loop not only ensures the machine's stability but also effectively mitigates noise. A comprehensive analysis is presented following a

comparison with the conventional proportional-integral controller.

## System Design

The system under consideration in this study is illustrated in Fig. 1. It comprises a singular power circuit accompanied by two intricate control loops. Within the power circuit, a variable voltage and frequency power source supplies the requisite energy to the induction motor, facilitating precise speed regulation. Meanwhile, the control circuit transmits switching pulses to the inverter of the power source, following a comparative analysis of the signals from the motor terminals and the reference signals. The two control loops are instrumental in decoupling torque and flux. In this investigation, the Proportional Integral Control principle has been initially employed to generate the reference torque,  $T^*$ , and the reference flux,  $\phi_m^*$ .

Additionally, noise represents a critical factor that must be integrated into the speed sensor and subsequently mitigated. Consequently, noise has been deliberately incorporated into the system to scrutinize and comprehend its influence on the machine's operation.

## Field-Oriented-Controlled Induction Machine

The dynamic model of induction motor, considering the  $d$ - $q$  model [18] of the machine in the reference frame rotating at synchronous speed  $\omega_e$ , can be explained as below :

$$v_{qs} = R_s i_{qs} + \frac{d\phi_{qs}}{dt} + \omega_e \phi_{ds} \quad (1)$$

$$v_{ds} = R_s i_{ds} + \frac{d\phi_{ds}}{dt} - \omega_e \phi_{qs} \quad (2)$$

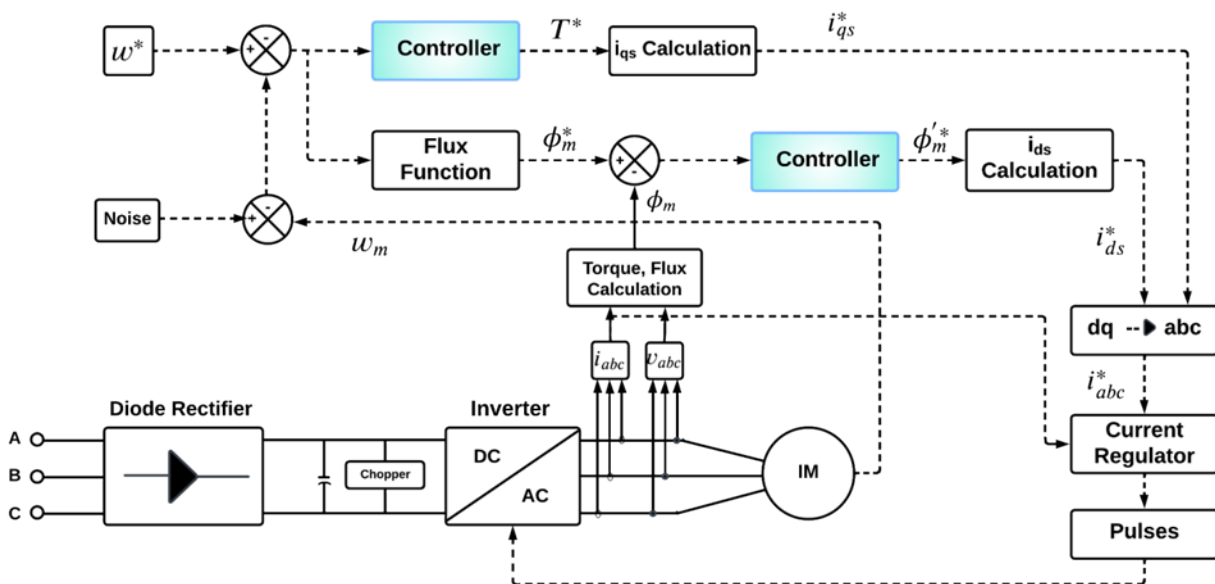


Fig. 1: Block Diagram of Field-Oriented-Controlled Induction Motor Drive System with Noise

For squirrel cage induction machine,  $v_{qr} = v_{dr} = 0$ , thus

$$v_{qr} = 0 = R_r i_{qr} + \frac{d\phi_{qr}}{dt} + (\omega_e - \omega_r) \phi_{dr} \quad (3)$$

$$v_{dr} = 0 = R_r i_{dr} + \frac{d\phi_{dr}}{dt} - (\omega_e - \omega_r) \phi_{qr} \quad (4)$$

and the equation of electromagnetic torque,  $T_e$  produced in the induction motor is given as

$$T_e = 1.5 p \frac{L_m}{L_r} (\phi_{dr} i_{qs} - \phi_{qr} i_{ds}) \quad (5)$$

where,

$$\phi_{qs} = L_s i_{qs} + L_m i_{qr} \quad (6)$$

$$\phi_{ds} = L_s i_{ds} + L_m i_{dr} \quad (7)$$

$$\phi_{qr} = L_r i_{qr} + L_m i_{qs} \quad (8)$$

$$\phi_{dr} = L_r i_{dr} + L_m i_{ds} \quad (9)$$

where,

$v_{qs}$  = quadrature axis stator voltage,  $v_{ds}$  = direct axis stator voltage,  $v_{qr}$  = quadrature axis rotor voltage,  $v_{dr}$  = direct axis rotor voltage,  $R_s$  = stator winding resistance,  $L_s$  = stator winding leakage inductance,  $L_m$  = magnetizing inductance,  $R_r$  = rotor winding resistance referred to the stator,  $L_r$  = rotor winding leakage inductance referred to the stator,  $\omega_e$  = synchronous speed with respect to  $d^s - q^s$  axes,  $\omega_r$  = rotor speed,  $p$  = number of pole pair,  $\phi_{qs}$  = quadrature axis stator flux,  $\phi_{ds}$  = direct axis stator flux,  $\phi_{qr}$  = quadrature axis rotor flux,  $\phi_{dr}$  = direct axis rotor flux

The speed  $\omega_r$  in equations (3) and (4) cannot normally be treated as a constant. It is related to the torque as

$$T_e = T_L + J \frac{d\omega_r}{dt} \quad (10)$$

where  $T_L$  = load torque, and  $J$  = moment of inertia of the machine.

Considering the rotor circuit equations (3) and (4),

$$R_r i_{qr} + \frac{d\phi_{qr}}{dt} + (\omega_e - \omega_r) \phi_{dr} = 0 \quad (11)$$

$$R_r i_{dr} + \frac{d\phi_{dr}}{dt} - (\omega_e - \omega_r) \phi_{qr} = 0 \quad (12)$$

From equations (8) and (9), we can write,

$$i_{qr} = \frac{1}{L_r} \phi_{qr} - \frac{L_m}{L_r} i_{qs} \quad (13)$$

$$\text{and } i_{dr} = \frac{1}{L_r} \phi_{dr} - \frac{L_m}{L_r} i_{ds} \quad (14)$$

Substituting for  $i_{qr}$  and  $i_{dr}$  in equations (11) and (12), we obtain

$$\frac{d\phi_{qr}}{dt} + \frac{R_r}{L_r} \phi_{qr} - \frac{L_m R_r}{L_r} i_{qs} + (\omega_e - \omega_r) \phi_{dr} = 0 \quad (15)$$

$$\frac{d\phi_{dr}}{dt} + \frac{R_r}{L_r} \phi_{dr} - \frac{L_m R_r}{L_r} i_{ds} + (\omega_e - \omega_r) \phi_{qr} = 0 \quad (16)$$

For decoupled control, we equate,

$$\phi_{qr} = 0 \quad (17)$$

$$\text{which implies, } \frac{d\phi_{qr}}{dt} = 0 \quad (18)$$

Now, the total rotor flux becomes,

$$\phi_r = \phi_{dr} \quad (19)$$

Substituting (17) and (19) in equations (15), (16) and (5), we get

$$(\omega_e - \omega_r) = \frac{L_m R_r}{\phi_r L_r} i_{qs} \quad (20)$$

$$\frac{d\phi_r}{dt} = -\frac{R_r}{L_r} \phi_r + \frac{L_m R_r}{L_r} i_{ds} \quad (21)$$

$$\text{and } T_e = 1.5 p \frac{L_m}{L_r} (\phi_r i_{qs}) \quad (22)$$

### Model Predictive Controller

Model Predictive Controller (MPC) is a feedback control algorithm that uses a model to make predictions about future outputs of a process [15-17]. It uses the model of a system to predict future plant output and solves an optimization problem to select the optimal control that is the closest to the predicted plant output. This allows MPC to account for the effects of noise and other disturbances in the system model which can improve its control performance. Also, MPC allows an easy incorporation of noise as compared to PI, allowing for better analysis of results.

The parameters of MPC include the Prediction Horizon ( $p$ ) and Control Horizon ( $m$ ). Prediction Horizon is how far it can look into the future i.e., the number of samples in the future for which the controller predicts the plant output. The Control Horizon is the number of samples within the prediction horizon where the controller can affect the control action.

The working of MPC can be explained in four steps :

#### • Observation of Model

The MPC requires a model which describes the input and output behavior of the process. The observer within it converts the model into a discrete state space model of the type,



$$x_c(m+1) = Ax_c(m) + Bu_o(m) \quad (23)$$

$$y(m) = Cx_c(m) + Du_o(m) \quad (24)$$

Where, at the  $m^{th}$  sample number

$x_c$  is the controller state

$u_o$  is the input to the model

$y$  is the output of the model  $a_b$

$A, B, C, D$  are state observer parameters

MPC controller uses the observed model in the following ways:

1. To estimate values of unmeasured states needed as the basis for predictions.
2. To predict how the controller's proposed variable adjustments will affect future plant output values.

### • State Estimation

It is a technique where the current state of the system is inferred based on a finite sequence of past measurements. State estimation is used to estimate the unmeasured states and provide the MPC controller with a more complete picture of the system's behavior. This estimated state is then used in the MPC algorithm to predict the future behavior of the system and to generate control actions. The controller uses a steady-state Kalman filter that derives from the state observer for the estimation.

At the beginning of the  $m^{th}$  control interval, the controller state is estimated with the steps listed below :

1. Calculation of the following data

$x_c(m|m-1)$  - Controller state estimate from previous control interval,  $m-1$

$u^{orig}(m-1)$  - Manipulated variable originally used in plant from  $m-1$  to  $m$

$u^{opt}(m-1)$  - Optimal manipulated variable recommended by MPC and assumed to be used in the plant from  $m-1$  to  $ma_b$

$d(m)$  - Current measured disturbances i.e. noise  $b$

$y_m(m)$  - Current measured plant outputs

$B_u, B_d$  - Columns of observer parameter  $B$  corresponding to  $u(m)$  and  $d(m)$  inputs

$C_k$  - Rows of observer parameter  $C$  corresponding to measured plant outputs

$D_{kd}$  - Rows and columns of observer parameter  $D$  corresponding to measured plant outputs and measured disturbance inputs

$L, M$  - Constraint Kalman gain matrices

2. Alter  $x_c(m|m-1)$  when  $u^{orig}(m-1)$  and  $u^{opt}(m-1)$  are not the same.

$$x_c^{new}(m|m-1) = x_c(m|m-1) + B_u \left[ u^{orig}(m-1) - u^{opt}(m-1) \right] \quad (25)$$

3. Calculate the change from the plant output.

$$c(m) = y_m(m) - [C_k x_c^{new}(m|m-1) + D_{kd} d(m)] \quad (26)$$

4. Revise the controller state estimate to consider the latest measurements.

$$x_c(m|m) = x_c^{new}(m|m-1) + Mc(m) \quad (27)$$

The MPC-recommended manipulated variable value to be used between control intervals  $m$  and  $m+1$  is calculated using the current state estimate,  $x_c(m|m)$  by solving the quadratic program at interval  $m$ .

### • Output Prediction

Output variable prediction in MPC involves predicting the future values of the system's output variables over a prediction horizon. These predicted output values are then used to generate a sequence of control actions to achieve desired control objectives.

The following parameters are required for the prediction of the output variable :

$p$  - Prediction horizon

$x_c(m|m)$  - Controller state estimates

$d(m)$  - Current measured disturbance inputs (MDs)

$d(m+i|m)$  - Projected future MDs, where  $i$  lies between 1 to  $p-1$

$A, B_u, B_d, C, D_d$  - State observer parameters

The predicted plant output is always noise-free. Thus, all terms involving the measurement noise states disappear from the state observer equations.

From the above data, the state observer predicts the first step as,

$$x_c(m+1|m) = Ax_c(m|m) + B_u u(m|m) + B_d d(m|m) \quad (28)$$

In general, the state observer prediction can be written as,

$$x_c(m+i|m) = Ax_c(m+i-1|m) + B_u u(m+i-1|m) + B_d d(m+i-1|m),$$

where  $i$  varies from 1 to  $p$ . (29)

Correspondingly, the predicted noise free plant output can be written as,

$$y(m+i|m) = Cx_c(m+i|m) + D_{kd} d(m+i|m), \quad (30)$$

where  $i$  varies from 1 to  $p$ .

### • Optimization

Optimization is a key component of MPC. In MPC, an optimization problem is solved at each control interval to generate the control actions that will drive the system towards the desired behavior while satisfying constraints. The optimization problem is typically formulated as a constrained quadratic program (QP), where the objective is to minimize a cost function that penalizes deviations from the desired behavior, subject to constraints on the system's inputs, outputs, and states.

The cost function in MPC typically includes a measure of the system performance, such as the tracking error between the system output and the desired setpoint, and penalties for deviations from desired operating conditions or constraints on the system inputs and outputs. The cost function is usually defined over a finite horizon, which represents the time interval over which the system behavior is predicted and optimized.

$$J = \sum_{m=0}^P (y_m - r)^T Q (y_m - r) + \sum_{m=0}^P \Delta u^T R \Delta u \quad (31)$$

Where,

$r$  - Setpoint

$\Delta u$  - Predicted change in control value

$Q$  - Output error weight matrix (positive semi-definite)

$R$  - Control weight matrix (positive definite)

### Parameters of Induction Machine

The parameters of the induction machine is given in this subsection. Also, these parameters have been verified using methods given in [19] and the error is less than 1%. The induction machine used is three-phase 440 V, 50 Hz, 4 poles, 220-hp motor with its calculated parameters are given below. Per phase stator resistance;  $R_s = 14.85 \times 10^{-3} \Omega$ , Per phase rotor resistance;  $R_r = 9.295 \times 10^{-3} \Omega$ , Per phase stator inductance;  $L_s = 0.3027 \times 10^{-3} \text{ H}$ , Per phase rotor inductance;  $L_r = 0.3027 \times 10^{-3} \text{ H}$ , Per phase mutual inductance;  $L_m = 10.46 \times 10^{-3} \text{ H}$ , and Moment of inertia of the rotor;  $J = 3.1 \text{ kg-m}^2$

## RESULTS AND DISCUSSIONS

The model of the system shown in Fig. 1 is developed and simulated in the MATLAB/Simulink environment using the dynamic modeling and parameters discussed in the previous section. The model is solved using a fixed step ode45 solver.

Initially, model has been developed using PI controller with values,  $K_p = 100$ ,  $K_i = 30$  and the improved model uses an MPC controller with parameters,  $p = 20$ ,  $m = 2$ ,  $T_s = 0.0001\text{s}$  for flux regulation. For the torque-reference generating PI controller the values for  $K_p$  and  $K_i$  are 300 and 2000 respectively and the values for the corresponding MPC controller are 20, 2 and 0.0001s for  $p$ ,  $m$  and  $T_s$  respectively. Simulated results of various important variables are given from Fig. 2 to Fig. 13

Fig. 2 shows the flux waveforms obtained using MPC and PI controllers without noise. It can be seen from the figure that the settling time obtained by the MPC is comparatively less than the PI controller which is a significant advantage. These results are without any noise in the measured speed, however the response of the controller deviates from accuracy when the measured is subjected to disturbance. A white noise of power 0.001 is added to the measured speed as shown in Fig.1 and then this disturbed speed is fed to the controller. The response of both the controllers are depicted in Fig. 3. It shows improved transient performance of the reference flux waveform. The predictive nature of MPC is responsible for this, as it can respond to changes in the system and quickly adjust the control inputs to minimize the impact of noise.

Fig. 4 further shows the effect of noise on the d-axis and q-axis flux. These flux waveforms exhibit considerable fluctuations and oscillations in the PI-controlled machine. In contrast, the MPC controller is able to effectively control the impact of noise on the q-axis and d-axis flux waveforms, resulting in better performance.

The d-axis and q-axis flux plotted against each other, independent of time can be seen in Fig. 5. It can be observed that they follow the principle of vector control i.e., the flux  $\phi_d$  and  $\phi_q$  are orthogonal to each other [6].

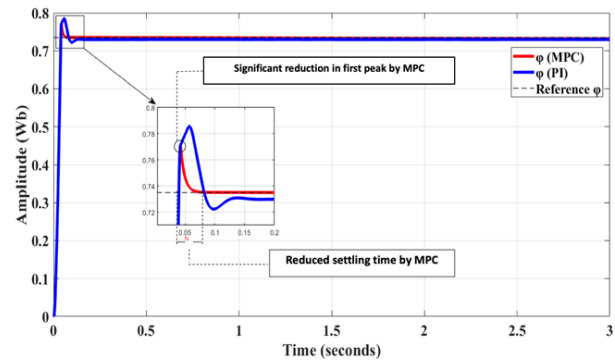


Fig. 2: Stator flux waveforms without noise in measured speed

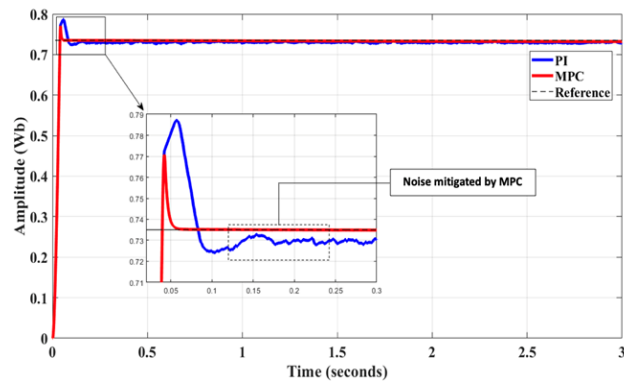


Fig. 3: Stator flux waveforms with noise in measured speed





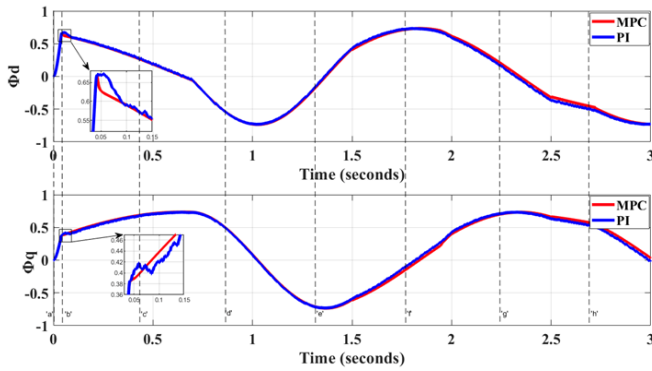


Fig. 4: (a) d-axis flux (b) q-axis flux

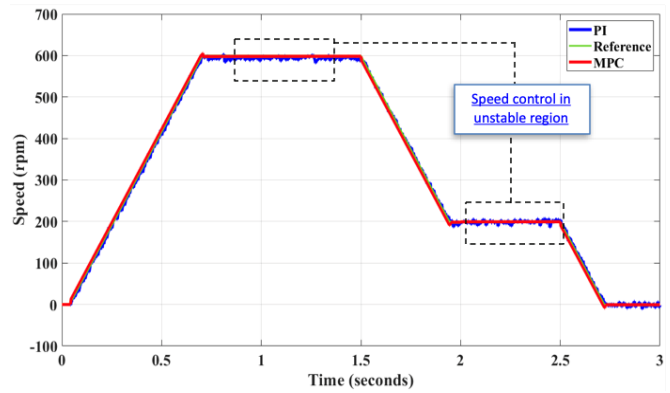
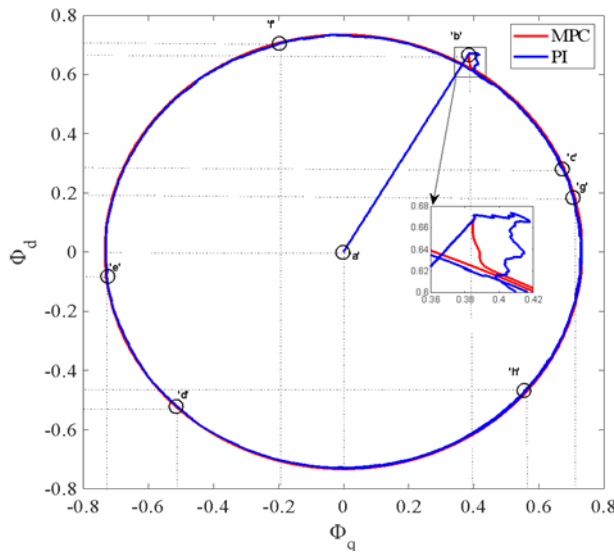


Fig. 6: Speed waveforms

Fig. 5:  $\phi_d$  vs  $\phi_q$  plot

The difference in speed waveforms obtained from MPC and PI can also be seen in Fig. 6. The MPC controller is capable of effectively controlling the impact of noise on the speed waveform and the result is a smooth waveform whereas the speed waveform obtained is sluggish with the PI controller.

As seen in Fig. 7, when the machine is subjected to noise, the reference-torque waveform obtained from the PI controller is severely affected which further affects the electromagnetic torque generated by the machine, making it unstable. Thus, the PI controller is incapable of generating the reference-torque as it leads to unstable operation of the machine.

In Fig. 8, the reference torque (in black) is obtained for the MPC controller, and it is visibly stable as compared to what was achieved from the PI controller (Fig. 7). The torque waveform obtained from the PI controller is highly oscillatory and deviates significantly from the reference torque waveform. On the other hand, the torque waveform obtained from the MPC controller follows the reference torque waveform more closely with slight ripples.

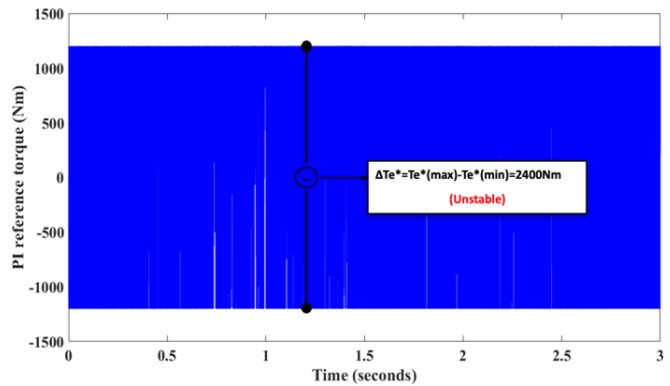


Fig. 7: Reference torque obtained by PI controller

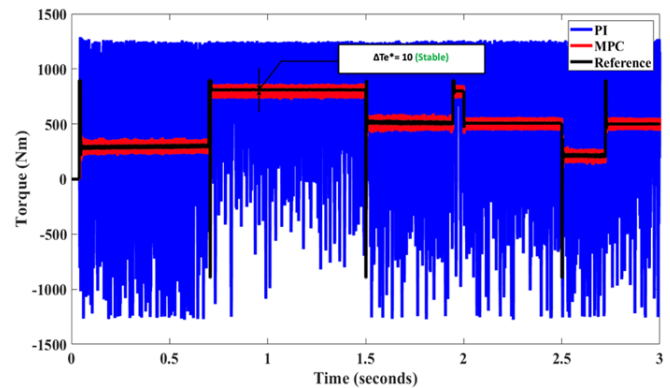


Fig. 8: Torque waveforms

Fig. 9 and Fig. 10 depicts the torque-speed characteristics of an induction machine obtained from a PI controller and an MPC controller respectively. It can be clearly seen that the torque-speed characteristics obtained from the PI controller exhibit significant variations and departures, which leads to unstable operation. However, the MPC controller can maintain the stability, even under noisy conditions, resulting in superior control performance.

The unstable operation of the drive system with the PI controller can also be understood through current

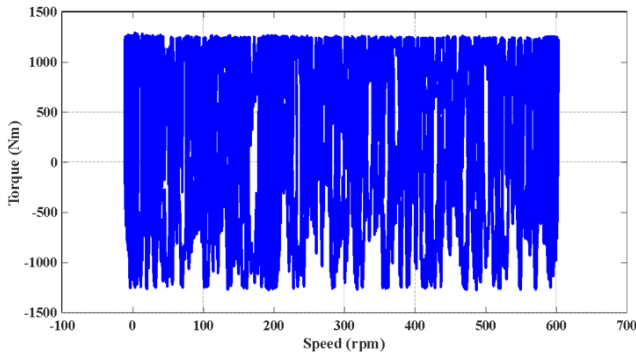


Fig. 9: Torque-speed characteristics of an induction machine obtained by PI controller

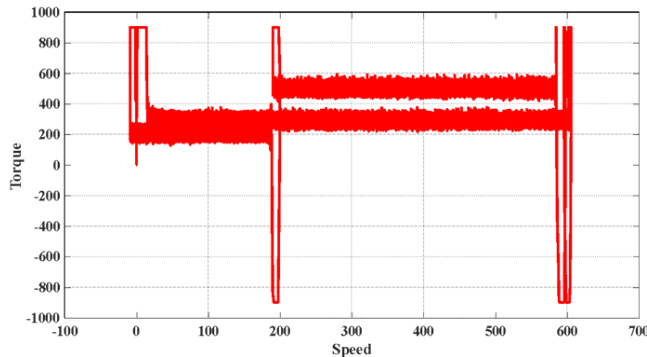


Fig. 10: Torque-speed characteristics of an induction machine obtained by MPC controller

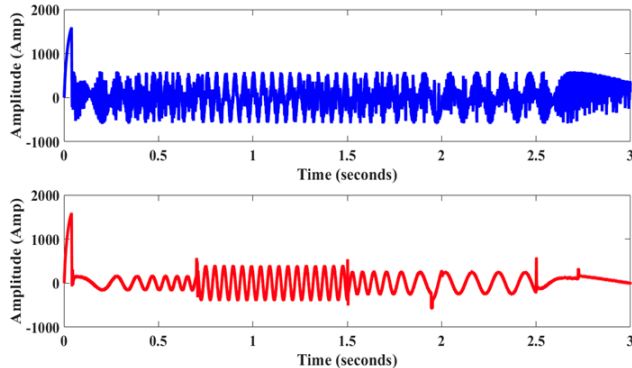


Fig. 11: Phase-a current waveform from (a) PI (b) MPC

waveforms. It can be seen in Fig. 11 that there is little impact of noise onto current obtained from the MPC controller, whereas its impact can clearly be seen on the current obtained from the PI controller.

The d-axis and q-axis current waveforms obtained from the PI and MPC controllers are shown in Fig. 12 and Fig. 13, respectively. It can be observed that the MPC controller is able to regulate the d-axis and q-axis current more precisely compared to the PI controller.

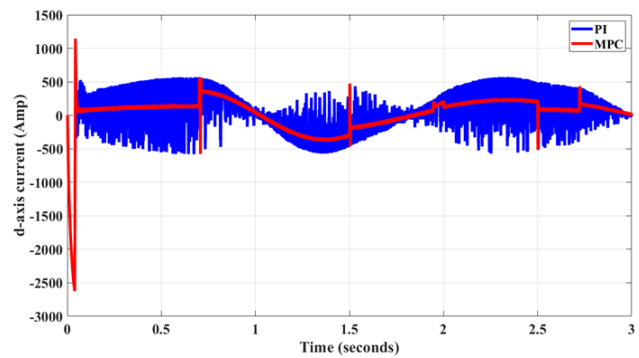


Fig. 12: d-axis current waveform

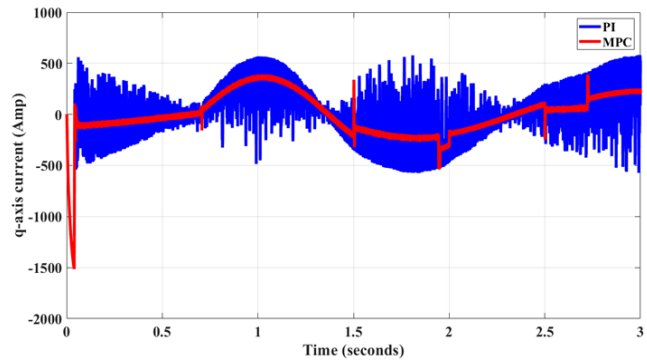


Fig. 13: q-axis current waveform

## CONCLUSIONS AND FUTURE SCOPE

In this work, a field-oriented-controlled induction motor drive system has been modeled in the MATLAB/Simulink environment in which two controllers have been applied, one on the reference-torque generator and another on the reference-flux generator. Initially, the controller used is a conventional Proportional Integral (PI) controller. Noise is incorporated into this system through a speed sensor. To improve the performance of the machine, a Model Predictive Controller is used in place of PI. The MPC controller improves the performance by employing advanced predictive algorithms, enabling it to anticipate system dynamics and optimize control actions accordingly. Comparative analysis of these two controllers in concluded form is:

### Stable Reference-Torque Generation

The implementation of the Model Predictive Controller (MPC) in place of the conventional Proportional-Integral (PI) controller addressed the challenges encountered by the latter in generating a stable reference-torque in the presence of noise. The MPC controller shows superior noise rejection capabilities and effectively mitigates the noise on the torque reference generation process. Consequently, the MPC controller provides a robust and stable reference torque thus ensuring reliable operation of the field-oriented-controlled induction machine drive system.

## Enhanced Transient Response of Flux Waveform

The conventional PI flux controller exhibits suboptimal transient response characteristics which results in prolonged settling times and elevated first transient peaks in the flux waveform. By replacing the PI flux controller with the MPC controller, significant improvements in transient response are achieved. As a result, the settling time and the amplitude of the first transient peak of the flux waveform are significantly reduced. This improvement in transient response enhances the dynamic performance of the field-oriented-controlled induction machine drive system.

The control technique described in this work has been developed using MATLAB/Simulink. A potential area for future exploration and enhancement is to implement the control in real time, which would help accelerate its commercialization process.

## REFERENCES

- [1] Le-Huy, H. (1999). Comparison of field-oriented control and direct torque control for induction motor drives. *Conference Record of the IEEE Industry Applications Conference. Thirty-Fourth IAS Annual Meeting*, 2, 1245–1252. <https://doi.org/10.1109/IAS.1999.805837>
- [2] Haq, H. U., Imran, M. H., Okumus, H. I., & Habibullah, M. (2015). Speed control of induction motor using FOC method. *International Journal of Engineering Research and Applications*, 5(3, Part 1), 154–158.
- [3] Petersson, A., Harnefors, L., & Thiringer, T. (2004). Comparison between stator-flux and grid-flux-oriented rotor current control of doubly-fed induction generators. *Proceedings of the 2004 IEEE 35th Annual Power Electronics Specialists Conference*, 1, 482–486. <https://doi.org/10.1109/PESC.2004.1355546>
- [4] Liang, Y., Xie, Y., Guan, Y., Lin, A., & Cheng, L. (2017). Comparison of the performance between stationary frame and synchronous rotating frame control of single-phase grid-connected inverter with LCL filter. *IEEE Conference on Energy Internet and Energy System Integration (EI2)*. <https://doi.org/10.1109/EI2.2017.8245633>
- [5] Krause, P. C. (2020). *Reference frame theory: Development and applications*. Wiley-IEEE Press.
- [6] Krishnan, R. (2001). *Electric motor drives: Modeling, analysis, and control*. Prentice-Hall.
- [7] Pahwa, V., & Sandhu, K. S. (2009). Transient analysis of three phase induction machine using different reference frames. *ARPN Journal of Engineering and Applied Sciences*, 4(8).
- [8] Ramsden, E. (2006). *Hall-effect sensors: Theory and applications* (2nd ed.). Elsevier.
- [9] Briz, F., Cancellas, J. A., & Diez, A. (1994). Speed measurement using rotary encoders for high performance AC drives. *Proceedings of IECON'94 - 20th Annual Conference of IEEE Industrial Electronics*, 1, 538–542. <https://doi.org/10.1109/IECON.1994.396059>
- [10] Ferreira, F. J. T. E., & Lopes, F. J. P. (2016). Webcam-based tachometer for in-field induction motor load estimation. *2016 XXII International Conference on Electrical Machines (ICEM)*, 2380–2388. <https://doi.org/10.1109/ICELMACH.2016.7732801>
- [11] Zellouma, D., Bekakra, Y., & Benbouhenni, H. (2023). Field-oriented control based on parallel proportional–integral controllers of induction motor drive. *Energy Reports*, 9, 611–620. <https://doi.org/10.1016/j.egy.2023.01.089>
- [12] Hanif, O., & Kedia, V. (2018). Evolution of proportional integral derivative controller. *2018 International Conference on Recent Innovations in Electrical, Electronics & Communication Engineering (ICRIEECE)*, 2655–2659. <https://doi.org/10.1109/ICRIEECE44171.2018.9009032>
- [13] Shtessel, Y., Edwards, C., Fridman, L., & Levant, A. (2013). *Sliding mode control and observation*. Birkhäuser.
- [14] Bordonì, U., & D'Amico, A. (1990). Noise in sensors. *Sensors and Actuators A: Physical*, 27(1–3), 17–24. [https://doi.org/10.1016/0924-4247\(90\)85003-F](https://doi.org/10.1016/0924-4247(90)85003-F)
- [15] Wang, C., Ohsumi, A., & Djurovic, I. (2002). Model predictive control of noisy plants using Kalman predictor and filter. *IEEE Region 10 Conference on Computers, Communications, Control and Power Engineering (TENCON'02)*. <https://doi.org/10.1109/TENCON.2002.1182632>
- [16] Short, M. (2015). A simplified approach to multivariable model predictive control. *International Journal of Engineering and Technology Innovation*, 5(1), 19–32.
- [17] Nakagaki, Y., & Zhai, G. (2020). A study on optimization algorithms in MPC. *Journal of Physics: Conference Series*, 1490, 012073. <https://doi.org/10.1088/1742-6596/1490/1/012073>
- [18] Wasynczuk, O., Sudhoff, S. D., Pekarek, S. D., & Krause, P. C. (2013). *Analysis of electric machinery and drive systems* (Vol. 75). Wiley-IEEE Press.
- [19] Pedra, J. (2008). On the determination of induction motor parameters from manufacturer data for electromagnetic transient programs. *IEEE Transactions on Power Systems*, 23(4), 1709–1718. <https://doi.org/10.1109/TPWRS.2008.2002283>